

MODELING OF DNA TRANSPORT IN VISCOELASTIC ELECTRO-HYDRODYNAMIC FLOWS FOR ENHANCED SIZE SEPARATION

B. Chami¹, M. Socol¹, M. Manghi², and A. Bancaud^{1}*

SUPPLEMENTARY MATERIAL:

Supplementary Material 1:

The hydraulic resistance of the chip:

The microchannel geometry, of rectangular cross section, with two different depths, $h_1=16\ \mu\text{m}$ and $h_2=2\ \mu\text{m}$ is represented in Fig. S7. Two different funnel geometries are present in the same chip, a linear shape of $m=1$ and a power-law shape of $m=2.5$ or 3 (Fig. S7 left and right), respectively. The width of the funnel at a position $w(x)$ is described by $w(x)/w_0 = (x/x_0)^m + 1$, where w_0 is the width of the constriction equal to $5\ \mu\text{m}$.

The hydraulic resistance R_h of a rectangular cross-section is given by Eq. (21), where L is the length of the channel.

$$R_h \approx \frac{12\eta L}{wh^3\left(1 - \frac{0.63h}{w}\right)} \quad (21)$$

In the funnel region, the hydraulic resistance is given by:

$$R_{h_funnel} \approx \int \frac{12\eta dx}{w_0 \left[\left(\frac{x}{x_0} \right)^m + 1 \right] h_2^3 - 0.63h_2^4} \quad (22)$$

The hydrodynamic and electrophoretic velocities are derived using the nominal inputs of the experiments, namely the pressure and voltage, respectively.

Hydrodynamic speed:

The hydrodynamic velocity can be obtained by evaluating the flow rate Q given by Eq. (23) where ΔP is the applied pressure difference and R_{h_total} , the total hydraulic resistance of the channel:

$$Q = \frac{\Delta P}{R_{h_total}} \quad (23)$$

The maximum hydrodynamic velocity of the Poiseuille profile $V_{p_0}(x)$ in the region of interest, the funnel, can be derived from the flow rate using the following relation:

$$Q = \frac{\Delta P}{R_{h_total}} = \frac{2}{3} h_2 w_0 \left[\left(\frac{x}{x_0} \right)^m + 1 \right] V_{p_0}(x) \quad (24)$$

Therefore, the hydrodynamic velocity is proportional to the applied pressure difference as shown by Eq. (25):

$$V_{p_0}(x) = \frac{3\Delta P}{2h_2w_0\left[\left(\frac{x}{x_0}\right)^m + 1\right]R_{h_total}} \quad (25)$$

Electrophoretic speed:

The electrophoretic velocity V_e can be derived from the electric field E using Gauss' law of conservation of electric flux Φ along a cross-section S (Eq.(26)) and the Gradient theorem (Eq. (27)):

$$\Phi = \oiint \vec{E} \cdot \vec{dS} \quad (26)$$

$$V(\vec{a}) - V(\vec{b}) = - \int_a^b \vec{E} \cdot \vec{dl} \quad (27)$$

where $V(\vec{a})$ and $V(\vec{b})$ is the electric potential at points a and b , respectively and l the distance between the two points.

In the funnel region, the electric field at a given position in KV/m is given by:

$$E(x) \approx \frac{\alpha\Delta V}{w_0\left[\left(\frac{x}{x_0}\right)^m + 1\right]} \quad (28)$$

where α is a dimensionless constant that depends on the funnel geometry.

Finally, the electrophoretic speed, at a given position in the funnel, can be obtained by multiplying the electric field with the electrophoretic mobility of DNA in a given polymer solution (Table1).

$$V_e(x) = \mu_e E(x) \quad (29)$$

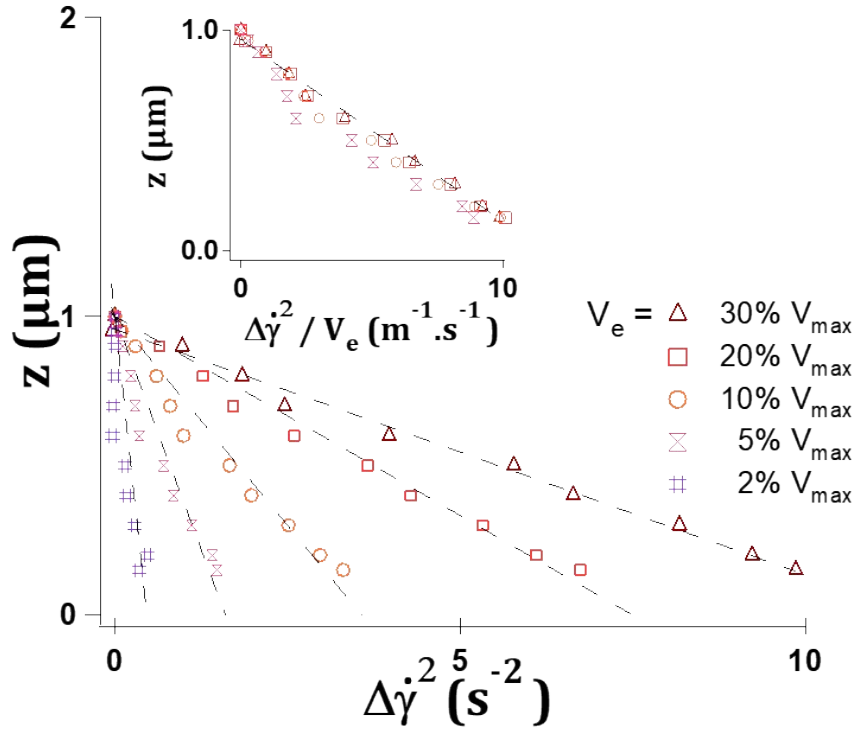


Figure S1: Transverse viscoelastic force finite element modeling. Using 3D finite element modeling, we determine the difference in square of the shear rate on the upper and lower apexes of the particle, as reported in the x axis of the graph.

The channel height h , particle radius a , and hydrodynamic maximum speed V^{p0} are set to $2 \mu\text{m}$, 50 nm , and $75 \mu\text{m/s}$, respectively with different electrophoretic velocities, as indicated in the legend. The set of data can be rescaled with the electrophoretic velocity (inset). Dashed lines correspond to guides to the eye.

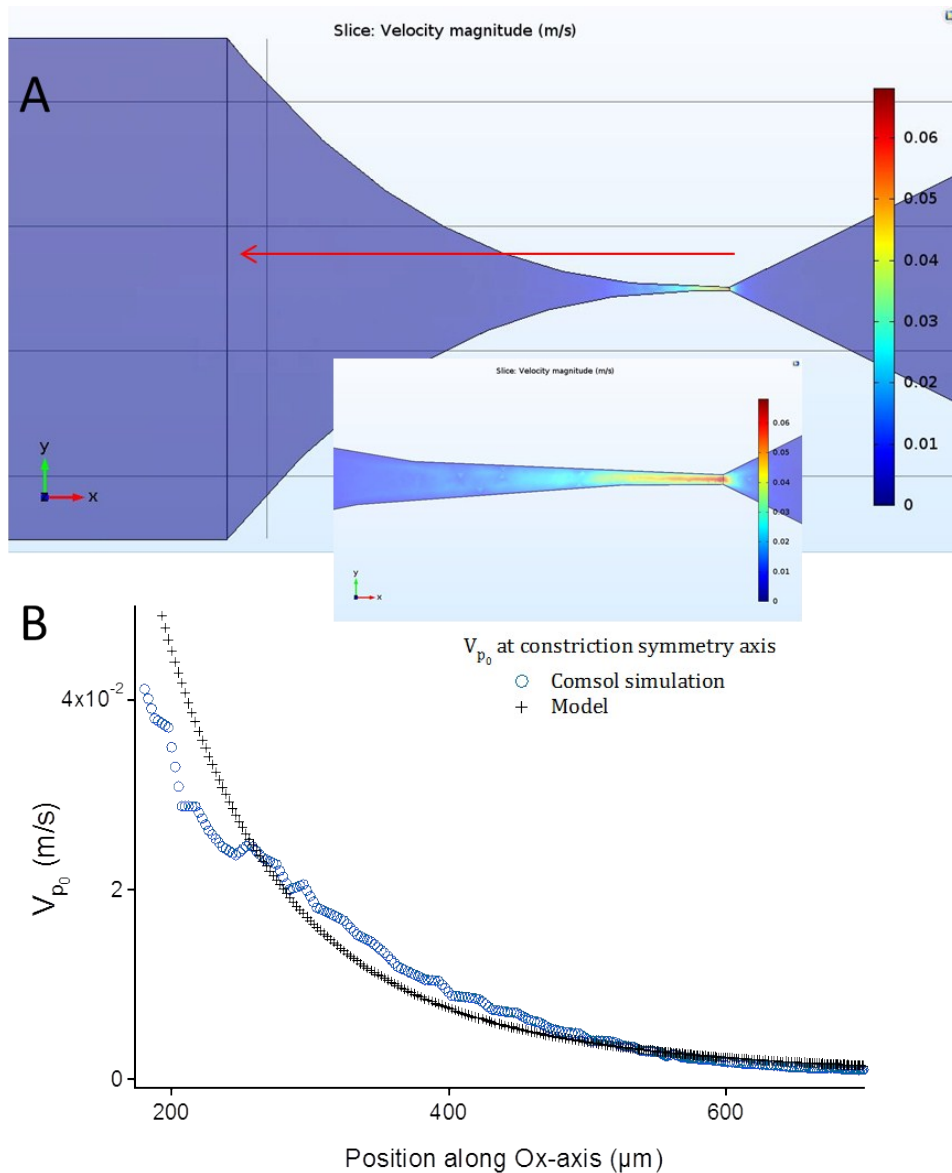


Figure S2: Validation of Eq. (11) by finite element modeling. (A) Using 3D finite element modeling, we determine the flow velocity in a funnel with a power-law shape characterized by $m=3$. (B) The maximum flow velocity inferred from the simulation along the channel symmetry axis is plotted as a function of the distance to the apex (red arrow in (A)) using blue circles. Our approximation in Eq. (11) is plotted with black crosses. Note that the comparison is drawn starting from 200 μm from the apex, because it corresponds to the position where the bands of 300 to 1000 bp accumulate (see e.g. Fig. 1).

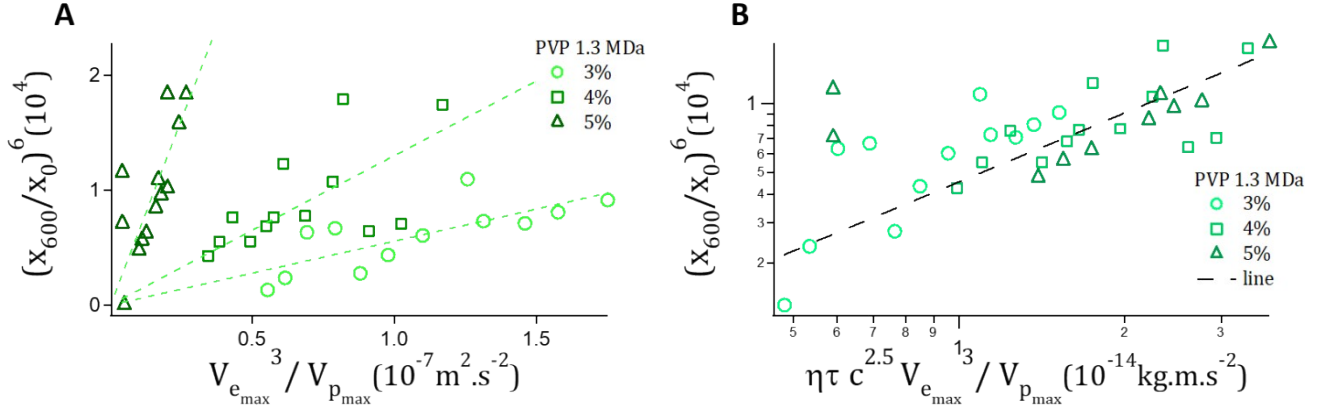


Figure S3: Analysis of the band position. (A) The position x_{600} of the band of 600 bp raised to the power $2m$ with $m=3$ is plotted as a function of $V_{e_{max}}^3/V_{p_{max}}$. We use a set of 1.3 MDa PVP concentrations, as indicated in the legends. (B) The datasets in (A) are normalized with the product $C_{PVP}^{2.5}\eta\tau$ in order to fall on to a master response.

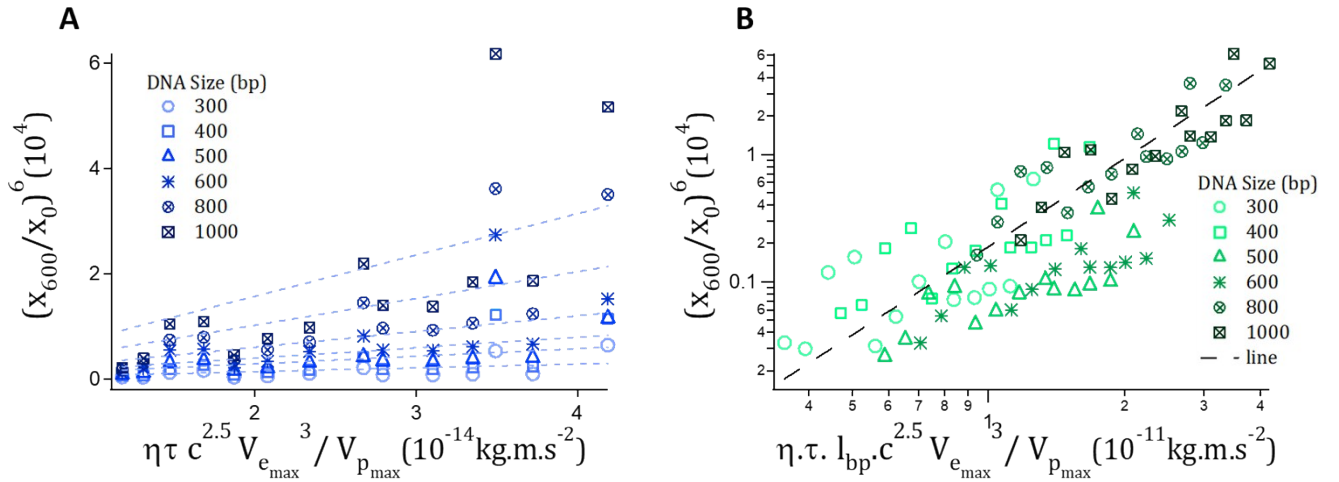


Figure S4: Size dependence of DNA band positions. (A) The plot represents the position of the bands of 300 to 1000 bp raised to the power $2m$ with $m=3$ as a function of $V_{e_{max}}^3/V_{p_{max}}$. (B) The same data is rescaled with the normalization factor $C_{PVP}^{2.5}\eta\tau$ and DNA contour length l_{bp} for the power law geometry.

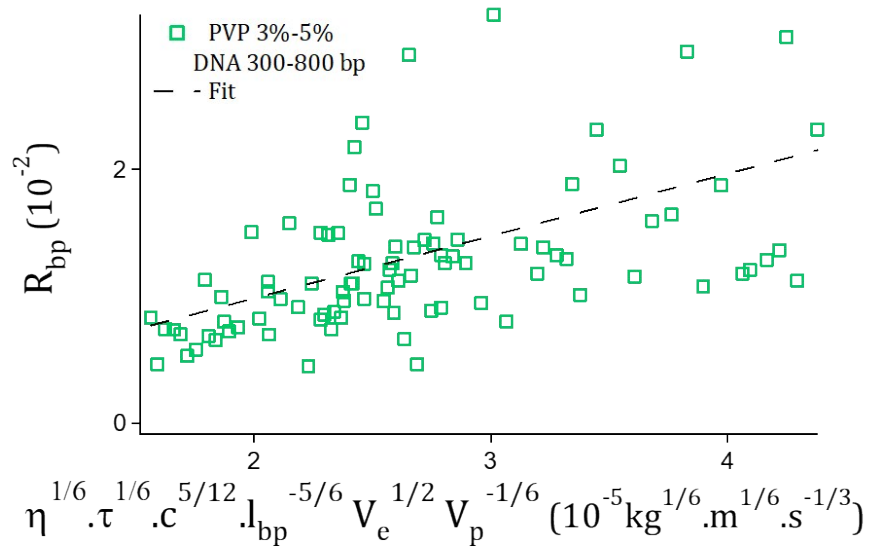


Figure S5: R_{bp} variation with DNA MW. The plot shows R_{bp} for different DNA stands of 300 to 1000 bp, for a power-law geometry ($m=3$). We use three different polymer concentrations (3%, 4% and 5% PVP 1.3 MDa).

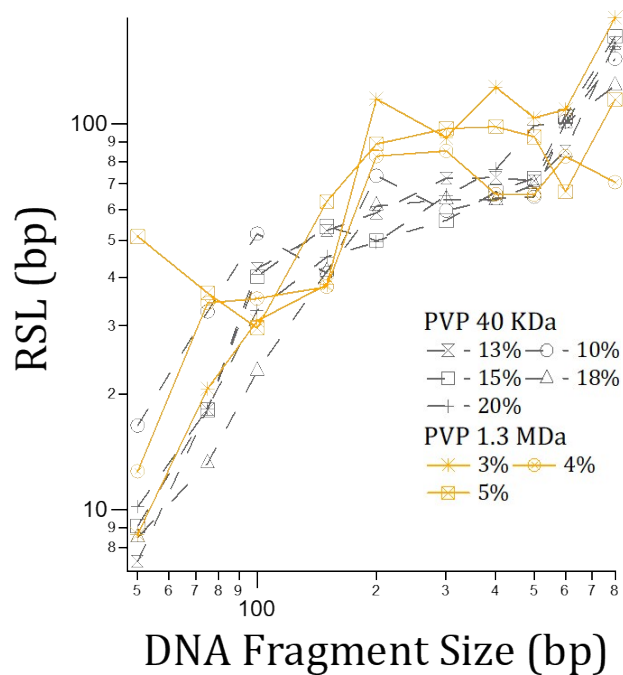


Figure S6: The RSL as a function of DNA size in different PVP solutions and concentrations. The graph shows the ability to reach 7 bp RSL for a 50 bp DNA band with PVP 40 KDa 13%.

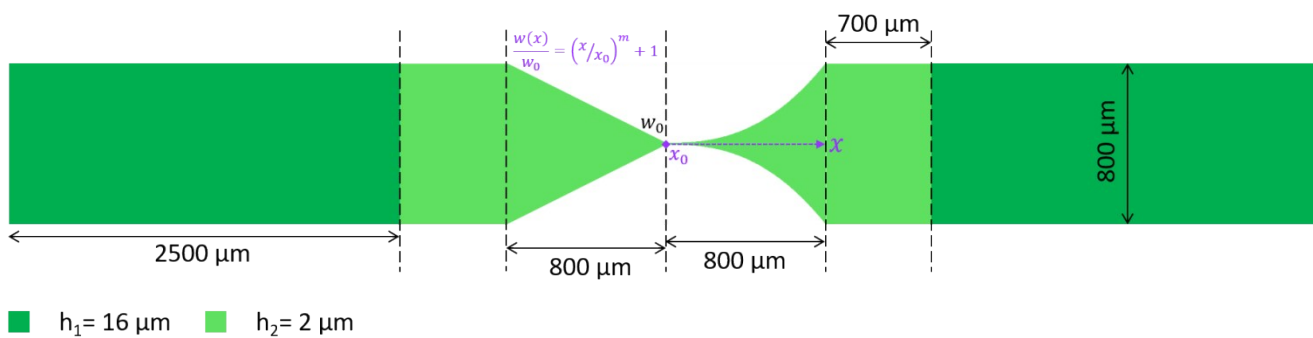


Figure S7: The microchannel geometry, of rectangular cross-section, containing two funnel shapes linear of $m=1$ and power-law of $m=2.5$ or 3 , to the left and right, respectively. The channel has two depths $h_1=16 \mu\text{m}$ and $h_2=2 \mu\text{m}$ represented in dark and light green, respectively.